Role of Calcium in the Adhesion and Fusion of Bilayers†

D. E. Leckband,‡ C. A. Helm,§ and J. Israelachvili*,‡

Department of Chemical and Nuclear Engineering, University of California, Santa Barbara, California 93106, and Institut für Physikalische Chemie, Johannes Gutenberg-Universität, Welderweg 11, D-6500 Mainz, Germany

Received March 27, 1992; Revised Manuscript Received September 30, 1992

ABSTRACT: The interaction forces and fusion mechanisms of mixed zwitterionic–anionic phospholipid bilayers were measured with the surface forces apparatus. The bilayers were 3:1 mixtures of either dimyristoylphosphatidylcholine and dimyristoylphosphatidylglycerol (DMPC/DMPG) or dilauroylphosphatidylcholine and dilauroylphosphatidylglycerol (DLPC/DLPG), and experiments were carried out in NaCl solutions with and without $CaCl_2$. In NaCl solutions, the forces between either mixed bilayer system were consistent with the DLVO (Derjaguin–Landau–Verwey–Overbeek) theory of repulsive electrostatic and attractive van der Waals forces, and fusion did not occur. At high pH (>6) and in high (20 mM) NaCl concentrations, a short-range hydration force extending about 13 Å was evident, indicative of Na^+ binding to the surfaces. In the presence of this large hydration repulsion, the interbilayer adhesion was abolished. When $CaCl_2$ was added to the bathing solutions in the presence or absence of NaCl, the bilayers phase separate into small domains, coinciding with the occurrence of a large, long-range attractive force. Fusion occurred readily between the more fluid domains. The phase separations and fusion events could be directly visualized by observing the shapes of the optical fringes used to measure the surface separation and the change in surface profiles with time. The ease of fusion between mixed bilayers in the presence of calcium correlated closely with the strength of the long-range attractive force. This force is attributed to the additional hydrophobic force between domains or domain boundaries due to the exposure of excess hydrophobic groups resulting from the Ca^{2+}-induced condensation of the PG^- headgroups. Fusion is, therefore, attributed to the enhanced hydrophobicity of phase-separated domains and only indirectly to ion binding, to an enhanced adhesion, or to dehydration effects. These results provide the first direct evidence of a molecular relationship between calcium-induced phase separation and bilayer fusion.

The role of cations in the adhesion and fusion of bilayers containing anionic lipids has been a topic of intensive study for many years (Papahadjopoulos et al., 1974, 1990; Papahadjopoulos, 1978; Poste & Nicolson, 1978; Düzgunes et al., 1984a,b; Sowers, 1987). Fusion is thought to occur as a result of a number of factors, most of which involve the close apposition of membranes due to a reduced interbilayer repulsion resulting from surface dehydration and/or interbilayer bridging by divalent ions (McIver, 1970; Portis et al., 1979, Parsegian & Rand, 1983; Rand & Parsegian, 1986; Feigenson, 1986; Leikin et al., 1987). Other factors that may reduce interbilayer repulsion are depletion attraction or dehydration induced by poly(ethylene glycol) (Boni & Hui, 1987), a reduction in repulsive interbilayer undulations by membrane tension, and osmotic stress effects (Evans & Metcalfe, 1984; Servuss & Helfrich, 1989). Bilayer fusion may also occur as a consequence of enhanced hydrophobic interactions between bilayers arising from lipid packing defects due to lateral phase separations, the formation of intrabilayer phase intermediates, membrane-bound proteins, or bilayer depletion (Papahadjopoulos et al., 1974; Papahadjopoulos, 1978; Siegel et al., 1989; Hui et al., 1981). It has been proposed, and recently demonstrated, that the increased hydrophobic attraction between stressed bilayers through exposure of the bilayer interior is a major driving force in the fusion mechanism (Ohki & Düzgunes, 1979; Ohki, 1982; Ohki & Ohshima, 1984; Helm et al., 1989).

In regard to the mechanism of fusion, vesicle fusion has been modeled as a two-step process (Bentz et al., 1983). The vesicles first aggregate, and in the second step, bilayer destabilization and fusion occur. Divalent ions have been proposed to induce fusion primarily through membrane destabilization by inducing lateral phase separation or phase transitions, both as a result of specific ion–lipid interactions (Nir et al., 1980; Düzgunes et al., 1981, 1984a,b). In contrast, monovalent ions play no role in bilayer fusion, but they affect the overall fusion kinetics by altering the electrostatic forces between bilayers (Bentz et al., 1983).

Calcium-induced lateral phase separation has been proposed as an intermediate in bilayer fusion for several years (Papahadjopoulos et al., 1974, 1977; Papahadjopoulos, 1978). Phase separations would result in packing fluctuations at domain boundaries, facilitating fusion by interaction of the exposed hydrophobic regions (Hui et al., 1981). The occurrence of lateral phase separations in mixed lipid bilayers has since been correlated with their fusion susceptibility (Leventis et al., 1986; Silvius & Gagne, 1984a; Hui et al., 1983). In particular, differential scanning calorimetry studies of mixed vesicles with homologous lipid chain lengths indicated that the appearance of macroscopic lateral phase separation correlates directly with increased fusion rates within certain composition ranges (Silvius & Gagne, 1984a, Hui et al., 1983). Other systems, however, undergo fusion at compositions where calcium does not induce macroscopic lateral phase separation (Silvius & Gagne, 1984b; Düzgunes et al., 1984a,b). In such cases, fusion has been attributed to the formation of microdomains, undectable by calorimetric measurements but observed by X-ray microprobe analysis and by ^{31}P-NMR (Hui et al., 1983). Additionally, it was also found that close

† D.E.L. was supported by NIH Grant PHS GM 47334, and C.A.H. was supported by NSF Grant CTS90-15537.

* To whom correspondence should be addressed.
‡ University of California.
§ Johannes Gutenberg-Universität.

0006-2960/93/0432-1127$04.00/0

apposition of membranes could also induce microdomain formation in the presence of calcium (Tokutomi et al., 1981). Consequently, membrane packing fluctuations in the region of intermembrane contact, as a result of calcium binding, are considered an important mechanism or intermediate in membrane fusion, though to date there have been no direct measurements which clarify the specific molecular mechanisms involved.

Monovalent ions also have a pronounced effect on fusion kinetics. At <100 mM NaCl, aggregation is rate determining, and fusion occurs readily following calcium-dependent vesicle aggregation. At high salt concentrations (>300 mM NaCl), fusion may not necessarily follow aggregation (Bentz et al., 1983). The behavior in both regimes suggests that competitive ion binding plays an important role in the overall fusion rate. In the presence of high NaCl concentrations, hydrated Na^+ ions bind to the surface, resulting in hydration thicknesses as large as 9 Å per bilayer surface (Claesson et al., 1989; Marra, 1986a; Loosley-Millman et al., 1982; Rand, 1981; Israelachvili, 1992). It is expected that such large interbilayer repulsive hydration forces significantly inhibit close apposition and adhesion of membranes (Rand & Parsegian, 1986; Leikin et al., 1987).

In the absence of ion binding, however, charged bilayer systems such as phosphatidylglycerol and dihexadecylphosphate (McIntosh et al., 1990; Marra, 1986a,b; Claesson et al., 1989; Pashley et al., 1986) do not exhibit any additional repulsive "hydration" force at separations greater than 5 Å.[1] In addition, the strongly repulsive electrostatic "double-layer" force between such charged surfaces under conditions of constant surface charge density is sufficiently strong to prevent them from coming close enough to adhere or fuse (Israelachvili & Wennerström, 1992).

In this work, the molecular interactions of mixed phosphatidylglycerol/phosphatidylcholine (PG/PC) bilayers were directly measured by use of the surface force apparatus. A 3:1 PC/PG mixture was utilized. This mixture was chosen because (i) PC and PG are common biological membrane lipids, and the 3:1 ratio is close to that found in some biological systems (e.g., in plant membranes), (ii) the relative 3:1 ratio of neutral to acidic lipids was used in a number of previous fusion studies of mixed lipids, and (iii) determined phase behavior indicates that the lipids should be miscible in both the solid and fluid phases (Findlay & Barton, 1978; this work).

In order to directly determine changes in the molecular interactions due to the introduction of calcium into the bathing medium, the interbilayer forces between fluid lipid bilayers were measured in both the presence and absence of $CaCl_2$. The fusogenic properties of the bilayers were measured, and the ease of fusion was correlated with the molecular forces manifested in the region where fusion occurred. The effects of the monovalent Na^+ ion were also examined to determine molecular mechanisms by which Na^+ can enhance or inhibit fusion in different concentration regimes. These measurements represent the first direct study of the actual molecular mechanisms of calcium-induced fusion of bilayer membranes.

MATERIALS AND METHODS

Dipalmitoylphosphatidylethanolamine (DPPE), dimyristoylphosphatidylcholine (DMPC), dimyristoylphosphatidylglycerol (DMPG), dilauroylphosphatidylcholine (DLPC), and dilauroylphosphatidylglycerol (DLPG) were purchased from Avanti Polar Lipids. Egg phosphatidylcholine and phosphatidylglycerol were from Sigma. $CaCl_2$ and NaCl were from Fluka. Ethylenediaminetetraacetic acid (EDTA) and *N*-tris[hydroxymethyl]methyl-2-aminoethanesulfonic acid (TES) were from Sigma. Water was doubly distilled and filtered through a Millipore Ultrapure system prior to use.

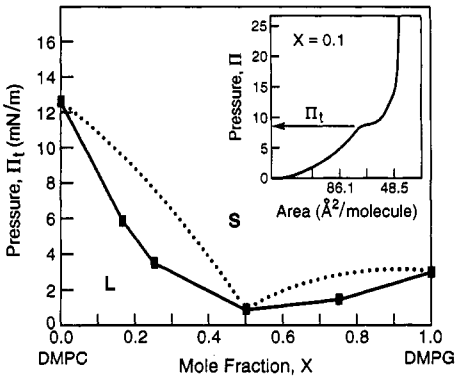

FIGURE 1: Dependence of the solid–liquid transition pressure of DMPC/DMPG mixtures on the mole fraction of DMPG. Monolayers of DMPC/DMPG mixtures with mole fractions varying from 0 to 1.0 were spread on a water subphase at 5 °C, and the transition pressures were determined from the breaks in the isotherms. A representative isotherm, taken/recorded at a mole fraction of X = 0.1, is shown in the inset. The phase diagram is indicated by the measured data (—) and the proposed solidus line by the dotted curves.

Aggregation of Mixed Lipid Vesicles in the Presence of Calcium. Large unilamellar vesicles of 3:1 egg PC/PG were prepared by the reverse-phase evaporation technique described elsewhere (Szoka & Papahadjopoulos, 1978). Aggregation was studied by following the change in absorbance at 350 nm upon addition of $CaCl_2$ in 2 mM TES at pH 7.0 to 1.0 mL to a solution consisting of 2 mM *N*-tris[hydroxymethyl]methyl-2-aminoethanesulfonic acid (TES), 20 or 100 mM NaCl, and 0.1 mg/mL lipid at pH 7.0 and 21 °C. The steady-state aggregation was followed by the time-dependent turbidity changes at 350 nm in a Beckman spectrophotometer (Szoka & Papahadjopoulos, 1978). Vesicle aggregation in the absence of calcium served as the control. The absorbance was read after a 45-min incubation at 21 °C. Previous work indicated that PG vesicles aggregate but do not fuse under these conditions (Szoka & Papahadjopoulos, 1978).

Film Balance Characterization of Mixed PG/PG Monolayers. Differential scanning calorimetric studies indicated complete miscibility of PG and PC in bulk solutions in the presence and absence of Ca^{2+} (Findlay & Barton, 1978). However, since monolayers at the air–water interface may not exhibit the same phase characteristics as bilayers in vesicles, it was necessary to determine the phase states of the mixed monolayers employed in these studies. The resulting data were used for preliminary indications of the phase state and molecular areas of the deposited lipids in this study. We note, however, that previous studies with vesicular systems demonstrated that calorimetry is not always a definitive indicator of phase behavior (Hui et al., 1983).

Monolayers of DMPC/DMPG mixtures were spread from a 9:1 chloroform/methanol solution at the air–water interface of a Teflon-coated Langmuir–Blodgett trough, and surface pressures were measured by the Willhelmy balance method. The composition of the mixtures was varied from 0 to 100% DMPG, and the solid–liquid transition pressures (Π_t) were measured as a function of the DMPC/DMPG ratio (Figure 1). In some cases, the subphase was 20 mM NaCl and 5 mM $CaCl_2$ at pH 5.6. The trough was equipped with a circulating water jacket for temperature control, and the water subphase

[1] Previous reports (Cowley et al., 1978) of a strongly repulsive hydration force between pure PG bilayers extending out to 30 Å were recently shown to be due to the expected electrostatic "double-layer" interaction (Israelachvili & Wennerström, 1992).

was cooled to 5 °C in order to observe the transitions of all the DMPC/DMPG mixtures. The transition pressures for DLPC/DLPG mixtures were measured at 7 °C on a subphase of 20 mM NaCl and 5 mM $CaCl_2$ at pH 5.6.

A series of calibration experiments were conducted to determine the surface pressure necessary to maintain the molecular area of the film during deposition onto a solid DPPE monolayer (molecular area 43 Å^2). The "transfer ratio", the ratio of area transferred to the area of the supporting surface, was determined at various surface pressures, and only those pressures yielding ratios of 0.96–1.04 were utilized in this work. This ensured that the molecular areas and, therefore, the composition of the transferred monolayers were identical to the monolayer on the water surface.

The most desirable molecular area for the deposition of the outer PC/PG layers was 65 Å^2/molecule since this is similar to the areas found in most biological membranes (Lis et al., 1982; MacDonald & Simon, 1987). Additionally, this ensures that the lipids will be in the fluid state in the absence of divalent ions (Marsh, 1990).

Force Measuring Apparatus. The surface force apparatus (SFA) used in these experiments has been described extensively elsewhere (Adams & Israelachvili, 1976; Marra & Israelachvili, 1985). The instrument in these studies was equipped with a variable spring which enabled the spring constant to be varied over 2 orders of magnitude. For dynamic measurements and recording of data, the optical system was interfaced with a videocamera recorder system equipped with a video micrometer and an internal timer. The occurrence of hemifusion was visualized with the optical interference technique described previously (Israelachvili, 1973; Helm et al., 1989, 1992). Briefly, the fringes of equal chromatic order (FECO), produced when white light is passed through the opposing sample surfaces, reflect the shape of the surface contact region. Thus, deformations in the elastic surfaces which occur in response to stresses on the system can be directly observed. The deformed shapes of contacting surfaces and thin films in response to different forces has been predicted theoretically and verified experimentally (Horn et al., 1987; Chen et al., 1991; Johnson et al., 1971); consequently, the FECO fringe patterns can be analyzed in terms of the repulsive or attractive forces acting between the surfaces. In the case where fusion occurs, local deformations are seen to occur at the point of lipid "breakthrough". These localized defects, which have a measured thickness equal to the thickness of a lipid bilayer, then increase in size as the hemifused region spreads laterally away from the initial breakthrough position (Helm et al., 1989, 1992). The change in the thickness of the two bilayers following hemifusion corresponds to the lateral diffusion of the two outer monolayers out of the contact region. Thus, a thickness change corresponding to the loss of two monolayers, or one bilayer, is used as another criterion for determining when and how rapidly hemifusion has occurred.

Preparation of Bilayer-Coated Mica Surfaces. The bilayers were supported on backsilvered mica sheets glued to fused silica discs. The discs were then transferred underwater to the measuring apparatus, as described elsewhere (Marra & Israelachvili, 1985), and mounted into the apparatus. Prior to introduction of the bilayer-coated discs, the apparatus was equilibrated with a saturated lipid solution containing either DMPC and DMPG or DLPC and DLPG at the desired salt composition for the experiment. Equilibration of the solution in the apparatus with the supported bilayer was necessary to prevent lipid desorption from the bilayer during experiments.

Supported bilayers were formed by deposition of monolayers of PC/PG mixtures onto solid monolayers of DPPE (43 Å^2/molecule) on mica. Monolayers of 3:1 DLPC/DLPG or 3:1 DMPC/DMPG mixtures in 9:1 chloroform/methanol were spread at the air–water interface of a Langmuir trough. The subphase in most experiments was water, but in some cases the subphase contained 20 mM NaCl and 5 mM $CaCl_2$. The temperature of the subphase was maintained at 25 °C. A layer of DPPE was transferred to the mica surface at a surface pressure of 38 mN/m (molecular area of 43 Å^2). For experimental sample preparations, 3:1 PC/PG monolayers were compressed to a molecular area of 65 Å^2 at 25 °C and transferred onto the solid DPPE monolayer by Langmuir–Blodgett deposition (Marra & Israelachvili, 1985).

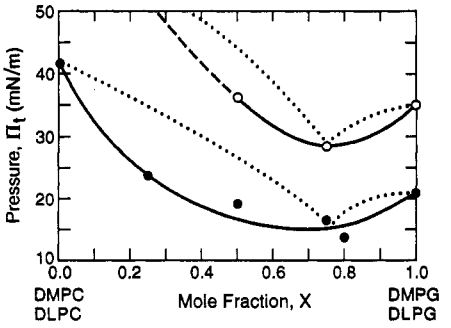

FIGURE 2: Solid–liquid transition pressures of DMPC/DMPG at 18 °C (●) and DLPC/DLPG at 7 °C (○). Monolayers were spread on a subphase of 20 mM NaCl and 5 mM $CaCl_2$ at pH 5.6. Solid lines indicate measured data, and broken lines refer to the proposed phase boundary.

RESULTS

Film Balance Studies. In order to determine the miscibility of solid DMPG with solid DMPC, the solid–liquid transition pressure was measured as a function of the fraction of PG in the monolayer. Mixed lipid films were spread at the air–water interface on a subphase maintained at 5 °C. The transition pressure–composition curve (Π_t–X) for the DMPG/DMPC mixture is shown in Figure 1, and a typical isotherm is shown in the inset. Transition pressures for pure DMPG and DMPC on a pure water subphase were 2.9 and 12.6 mN/m, respectively, at 5 °C. Π_t varied continuously with the mole fraction of DMPG. The liquidus curve (solid line) is similar to negative eutectic phase diagrams (Birdi, 1989), and the *hypothetical* solidus curve is indicated by the dotted lines. On the basis of the phase behavior indicated by the measured solidus curve, complete miscibility is expected in both the liquid (L) and solid (S) one-phase regions.

When the subphase contained 5 mM $CaCl_2$ and 20 mM NaCl (pH 6), the transition pressures were significantly lowered, but the dependence on the mole fraction of DMPG at 18 °C was similar (Figure 2, bottom curve). This behavior is similar to previous studies which demonstrated complete miscibility of DMPC and DMPG in the presence of calcium (Findlay & Barton, 1978). The transition pressures for the DLPC/DLPG mixtures on a NaCl/$CaCl_2$ subphase at 7 °C showed a similar trend (Figure 2, top curve), though the transition pressures at DLPG mole fractions less than 0.5 could not be accurately measured due to the weakness of the transition, i.e., the coexistence region of the isotherm was very small. Such transition behavior often occurs with lipids or lipid mixtures that do not exhibit a true first-order phase transition (Albrecht et al., 1981).

The surface pressures resulting in fidelity of transfer of the PC/PG monolayers onto a mica-supported monolayer of DPPE were determined. A transfer ratio of 1.0 is necessary to ensure that the composition and packing of the monolayer are maintained upon transfer to the support. On a pure water

Table I: Measured and Theoretical Bilayer Thicknesses

bilayer system	type of hydration	theoretical thickness[a] (Å)	experimentally measured thickness (Å)		
			X-ray diffraction[b]	SFA previous[c]	SFA this work[e]
		Fluid Phase ($T > T_t$)[d]			
DLPC (25 °C) in pure water	primary	32	30	30	
DMPC (27 °C) in pure water	primary	36	34.5	35	
3:1 DLPC/DLPG					
in pure water	primary	32			36
in NaCl solution	secondary	32			43
in $CaCl_2$ solution	unhydrated	32			30
		Frozen Phase ($T < T_t$)			
DMPC (10 °C) in water	primary	51	53		
DMPG (20 °C) in $CaCl_2$ solution	unhydrated	50	51		
3:1 DMPC/DMPG in $CaCl_2$ solution	unhydrated	50			51

[a] Unhydrated thickness only, calculated using eq 1 for a molecular area of $A = 65$ Å^2. [b] From Marsh (1990). [c] From Marra (1986a,b) and Marra and Israelachvili (1985). [d] T_t = solid–liquid transition temperature. [e] Hydrated thickness.

subphase at 25 °C and at a surface pressure of 35 mN/m (65 Å^2/molecule), the transfer ratios for both the DMPC/DMPG and DLPC/DLPG monolayers were 1.00 ± 0.04. If the subphase contained 20 mM NaCl and 5 mM $CaCl_2$ at 5 °C, the transition pressure is shifted for both mixtures. For the 3:1 DMPC/DMPG mixture, Π_t decreased to 17 mN/m at 18 °C. However, the transfer ratio obtained at the same molecular area of 65 Å^2 was again ~1.0.

Thickness of Bilayers and Definition of the Bilayer–Water Interface. The thickness of the outer monolayer on each surface, including its bound ions and associated water, was determined at the end of each experiment by measuring the thickness change following drainage of the solution from the apparatus and removal of the two outer monolayers. The thickness change Δ was measured relative to the distance of closest approach during the force measurements, and therefore corresponds to two lipid monolayers, or a single PC/PG bilayer, with its associated water and/or hydrated ions. In this paper, we refer to the surface-associated water as "primary" hydration and to water associated with adsorbed hydrated ions as "secondary" hydration, after Pashley (1981).

In the presence of calcium, the measured thickness changes were Δ = 51 ± 1 Å for DMPC/DMPG and Δ = 30 Å for DLPC/DLPG bilayers. In the absence of calcium, the thickness of the DLPC/DLPG bilayer was Δ = 36–43 Å, with increasing thickness occurring at higher NaCl concentrations (Table I). All depositions were at a molecular area of 65 Å^2. During experiments, the bilayer thickness was observed to increase (reversibly) on increasing the calcium or sodium ion concentration. Since it is unlikely that additional lipid becomes incorporated into the bilayers on changing the solution ionic strength, these thickness increases are attributed to ion binding of hydrated ions or to phase transitions and not to any changes in the average lateral headgroup areas.

The thicknesses of the lipid bilayers and corresponding hydration layers were determined as follows. We define the interbilayer separation at $D = 0$ as the contact between nominally dehydrated bilayers (Marra & Israelachvili, 1985) whose lipid volumes are given by theoretical equations (Tanford, 1972). In the absence of phase changes or lipid density changes, the thickness of the lipid monolayer is assumed to remain constant during each experiment due to conservation of volume. We first consider the fluid state, where the density of hydrocarbon chains is 0.70–0.75 g/cm^3. For fluid 12- and 14-carbon chains, therefore, the molecular volumes of C_{12} and C_{14} chains are $V_{hc} = 365$ and 436 Å^3, respectively (Marra, 1986b). The theoretical unhydrated bilayer thicknesses, D_b, is given by

$$D_b = 2(2V_{hc} + V_{head})/A \quad (1)$$

where V_{hc} is the average hydrocarbon chain volume, V_{head} is the average headgroup volume, and A is the deposited headgroup area. Using an average headgroup volume of $V_{head} = 318$ Å^3 for the 3:1 PC/PG mixture (Marra, 1985a), and the deposited molecular area of $A = 65$ Å^2, the theoretical thicknesses for fluid 12- and 14-carbon chain bilayers are $D_b = 32$ and 36 Å, respectively, in agreement with the X-ray diffraction (Marsh, 1990) and neutron reflectivity results (Bayerl et al., 1990) (Table I). The surface force apparatus (SFA)-measured thicknesses for the 12-carbon chain DLPC/DLPG bilayers were 36 Å in pure water, 43 Å in water containing NaCl, and 30 Å in the presence of $CaCl_2$ (Table I). The "unhydrated" DLPC/DLPG bilayer thickness of 30 Å measured in the presence of calcium is in good agreement with the measured 30 Å for pure DLPC obtained by neutron reflectivity, X-ray diffraction, and previous SFA measurements (Table I).

The steeply repulsive force at small separations which defined our distance of closest approach was attributed to such primary and secondary hydration or to a combination of hydration and steric effects (Israelachvili & Wennerström, 1991) and not to electrostatic forces, since the sharp upward breaks in the force laws (see later) did not correspond to any theoretical electrostatic force curves (Israelachvili, 1992). Referring to the last column of Table I, we thus find that the thicknesses of the primary and secondary hydration layers for the 3:1 DLPC/DLPG mixture are, respectively, (36 – 30) = 6 Å and (43 – 30) = 13 Å per bilayer. With the approach described here, the maximum hydration or Stern layer thickness occurred in the presence of NaCl and had a maximum value of 8 ± 2 Å per surface.

The thickness of the two outer DLPC/DLPG layers in the presence of calcium was 30 Å at 25 °C, similar to the theoretically predicted value for *fluid* bilayers and to that previously measured for DLPC bilayers (Marra & Israelachvili, 1985). Since no significant increase in thickness was measured, it was inferred that the DLPC/DLPG layers remained fluid in the presence of calcium, consistent with the phase diagram at this temperature (Figure 2).

Turning now to the frozen or gel-state bilayers, the unhydrated bilayer thickness is given by

$$D_b = 2[2(27.4 + 26.9n) + V_{head})]/A \quad (2)$$

where n is the number of methylene groups in the chain (Tanford, 1972). In the gel state, the molecular areas are

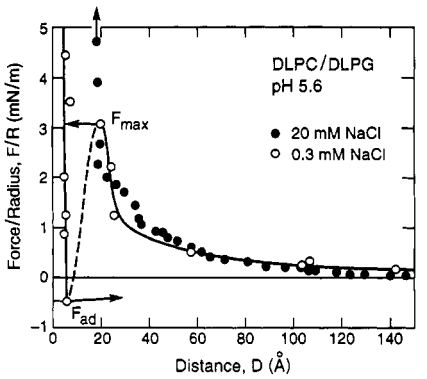

FIGURE 3: Forces between 3:1 DLPC/DLPG bilayers in 0.3 mM (○) and 20 mM (●) NaCl at pH 5.6 and 25 °C. In 0.3 mM NaCl, an adhesive minimum, due to van der Waals attraction, lies at $D \approx 4$ Å. The corresponding Hamaker constant was 7×10^{-21} J. Measured data at 0.3 mM NaCl are indicated by the solid line, and arrows at the force maximum (F_{max}) and minimum (F_{min}) indicate the jump-in and jump-off positions, respectively.

now 46 and 44 Å^2 for PC and PG, respectively (Helm et al., 1987; Marsh, 1990). Assuming an average volume V_{head} = 318 Å^3 for both the PC and PG headgroups, the theoretical thickness of the solid DMPC and DMPG bilayers are therefore 52 and 51 Å, respectively (Table I), in agreement with the value of 51 Å obtained for DMPG by X-ray diffraction (Table I). Equation 2, however, assumes a tilt angle of 0°. The thickness of 7:3 DMPC/DMPG monolayers at the air–water interface (pH 5.6) in the L_β (gel) phase was determined by neutron reflectivity to be 22.5 ± 1 Å (equivalent to a bilayer thickness of 45.0 Å) with a tilt angle of 32 ± 6° (Bayerl et al., 1990). Similarly, neutron reflectivity measurements also indicated the thickness of supported DMPC bilayers in the L_β phase to be 46 ± 1 Å with a tilt angle of 32° (Johnson et al., 1991). The DMPC/DMPG bilayer thicknesses reported here were obtained at pH 5.6 in the presence of calcium and were found to be 51 ± 2 Å. If the tilt angle is taken into account, the theoretical thickness would be 43 ± 3 Å. Given the errors and the reported differences in thicknesses obtained with the different techniques, our measurements may differ by as little as 3 Å (<1.5 Å per surface). Due the diffuse nature of the interface on such small length scales as well as uncertainties concerning the origin of hydration forces (Israelachvili & Wennerström, 1992), discrepancies of 3 Å are not considered to be of major significance. Nevertheless, our reported thickness of bilayers in the presence of calcium is significantly greater than that of DMPC/DMPG bilayers in the L_α phase and similar to the thickness of bilayers in the L_β phase (Bayerl et al., 1990). Consequently, the lipids do appear to undergo a phase transition in the presence of calcium. This is in contrast to the apparent phase behavior of the monolayers (Figure 2), which indicates miscibility in the presence of calcium. If this is the case, the previous assumption that the DMPG/DMPC bilayer thickness is determined by a frozen, presumably DMPG-rich phase is reasonable, since the thicker, solid DMPG-rich phase will determine the distance of closest approach for the mixed bilayers.

Interactions of DLPC/DLPG Bilayers in NaCl Solutions. In order to establish the surface forces in the absence of calcium, experiments were first conducted in NaCl and 10^{-4} M EDTA at pH 5.6, 7.4, and 8.8. TES buffer was included at 1 mM in the pH 7.4 solution, and EDTA was the only buffer in the pH 8.8 solution.

Figure 3 (open circles) shows the force profiles of interacting 3:1 DLPC/DLPG bilayers in 0.3 mM NaCl at pH 5.6. The long-range interaction was dominated by an exponentially repulsive force, similar to that expected for an electrostatic double-layer interaction at constant surface charge density. The measured exponential decay length was 167 Å, which compares well with the theoretical Debye length of κ^{-1} = 175 Å. At separations less than 20 Å, the surfaces undergo an instability due to the attractive van der Waals force and jump into adhesive contact at $D = 5 \pm 1$ Å. This behavior is consistent with DLVO theory.

From the measured adhesion or "pull-off" force, F_{ad}, the *adhesion energy* per unit area, E_{ad}, which by definition is also the depth of the potential energy minimum below $E = 0$ for two planar surfaces, can be determined from (Chen et al., 1991)

$$E_{ad} = -2F_{ad}/3\pi R \quad (3)$$

where R is the cylindrical radius of the mica surfaces. For the adhesive minimum at $D = 5 \pm 1$ Å in Figure 3, we obtain $E_{ad} = 0.5/1.5\pi = 0.1$ mJ/m^2. This energy, however, is not the same as the van der Waals energy E_{vdw}, at this separation. To obtain the van der Waals contribution we must subtract the repulsive electrostatic double-layer contribution, E_{el}, at this separation. The van der Waals energy is therefore given by

$$E_{vdw} \approx E_{max} + E_{ad} \quad (4)$$

Thus, referring to Figure 3, we obtain $E_{vdw} \approx 3.6/1.5\pi = 0.76$ mJ/m^2. The nonretarded Hamaker constant, A, is related to E_{vdw} by (Marra and Israelachvili, 1986)

$$E_{vdw} = A/12\pi\Delta D^2 \quad (5)$$

where ΔD is the distance of the adhesive minimum from the van der Waals plane of origin. The Hamaker constant for the mixed DLPC/DLPG layers, assuming that the van der Waals plane lies at $D = 0$ (ΔD = 0.5 nm), was thus determined to be $A = 12\pi E_{vdw}\Delta D^2 = 7 \times 10^{-21}$ J, in agreement with previously measured values for lipid bilayers interacting across water and about 50% higher than values calculated for hydrocarbon across water. The higher value can be attributed to the additional contributions arising from the more polar headgroups (Israelachvili, 1992). The value of 7×10^{-21} J is also slightly higher than values reported for some lipids (McIntosh et al., 1990), but we should note that, in all cases, interpretations of these types of measurements suffer from ambiguities in determining where the true van der Waals plane of origin lies (i.e., in knowing ΔD).

For interacting double layers in a 1:1 electrolyte at large separations (2–3 Debye lengths, κ^{-1}), the surface potential can be approximated by (Adams & Israelachvili, 1976; Hunter, 1989)

$$\psi_o = \frac{4kT}{e} \tanh^{-1} (F(D)\kappa e^{\kappa D}/128\pi nRkT)^{1/2} \quad (6)$$

where ψ_o is the surface potential in millivolts, κ is the reciprocal Debye length in reciprocal meters, k is the Boltzmann constant, n is the number density of counterions in the bulk phase, e is the electronic charge, and T is the absolute temperature. At 0.3 mM NaCl and pH 5.6, the measured surface potential was −36 mV (Table II). The effective surface charge density σ_{eff} is obtained from the Graham equation (Israelachvili, 1992)

$$\sigma_{eff}^2 = 4\epsilon_o\epsilon kT[\text{NaCl}]\{\cosh(e\psi_o/kT) - 1\} \quad (7)$$

where ϵ is the medium dielectric constant and [NaCl] is the salt concentration in units of molecules per cubic decimeter. The corresponding charge density at 0.3 mM NaCl and pH 5.6 (Figure 3) was $\sigma_{eff} = 1.4 \times 10^{-3}$ cm^{-2}, which corresponds to ~12 000 Å^2/charge (Table II, top row). Since the PG surface coverage is 260 Å^2/PG, this value further implies an

Table II: Double-Layer Parameters for DLPC/DLPG Bilayers at 25 °C[a]

pH	NaCl (mM)	λ_D[b] (Å)	λ_{th}[c] (Å)	Ψ (mV)	charge/Å^2 (×10^{-4})	Å^2/charge	α[d]
5.6	0.3	167	176	−36	0.86	11600	0.022
5.6	20	22	21	−31	6.71	1500	0.17
7.4	0.5	144	136	−47	1.75	5700	
7.4	21	21	21	−27	5.88	1700	

[a] Data from Figures 3–5. [b] $\lambda_D = \kappa^{-1}$ = measured Debye length. [c] λ_{th} = theoretical Debye length. [d] α = degree of dissociation (Å^2 occupied per PG molecule/Å^2 per charge).

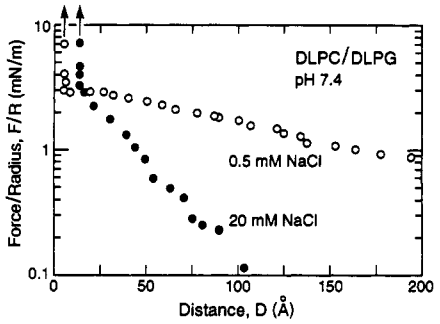

FIGURE 4: Forces between 3:1 DLPC/DLPG bilayers in 0.5 mM (○) and 20 mM (●) NaCl at pH 7.4 and 25 °C. Measurements of the bilayer interactions at 0.5 mM NaCl were followed by addition of NaCl at pH 7.4 to a final concentration of 20 mM.

effective degree of ionization of $\alpha = 260/12\,000 = 0.022$, or 2.2%.

At 20 mM NaCl and pH 5.6 (Figure 3, black circles), the force curve was dominated by electrostatic repulsion with a decay length of 22 Å, consistent with the theoretical Debye length of 21 Å (Table II). The surfaces did not adhere, indicating that the interactions were dominated by repulsive electrostatic and steric hydration forces. Furthermore, the sharp repulsion at $D \approx 16$ Å indicates that as a consequence of the increased Na^+ ion binding in 20 mM NaCl the thickness of the (secondary) hydration layer had increased to 8 Å per surface. At 20 mM NaCl and pH 5.6, the surface potential was −31 mV and the effective charge density was 1500 Å^2/charge, which corresponds to $\alpha = 0.17$ (Table II, second row).

At forces greater than 4–8 mN/m, the surfaces begin to locally deform (flatten) rather than move closer in (Adams & Israelachvili, 1976). Under such conditions where flattening occurs, the force per unit area or pressure ($P = F/\text{area}$) is reported. However, except where strongly repulsive short-range steric–hydration forces were encountered (cf. Figure 3, vertical arrow), no such deformations occurred until after the surfaces had surmounted the force barriers (which was typically at F/R values below 4 mN/m) and had "jumped" into strongly adhesive contact.

In 0.5 mM NaCl and 1 mM TES at pH 7.4 (Figure 4, open circles), the interaction is dominated by a long-range electrostatic repulsion with a 142-Å decay length ($\lambda_{theoret} = 136$ Å), and again no bilayer adhesion was detected. The calculated surface potential was −47 mV and the area per charge was 5700 Å^2/charge (Table II, third row). At pH 7.4, when the NaCl is increased to 20 mM (Figure 4, black circles), a large hydration force—attributed to primary and secondary hydration—is evident at separations less than 13 ± 3 Å. This repulsion dominates the short-range interaction and is consistent with previous observations in high monovalent electrolyte solutions at high pH (Marra, 1986a; Claesson et al., 1989). The electrostatic decay length decreased in a predictable manner (Table II, fourth row). No significant change in the surface potential accompanied the pH increase from 5.6 to 7.4.

Table III: pH and NaCl Concentration Dependence of Steric Hydration Force Layer and Adhesion Energies[a]

NaCl (mM)	$CaCl_2$ (mM)	pH	D_h (Å)	γ (mJ/m^2)
0.3	0.0	5.6	5	0.38
20	0.0	5.6	16 ± 3	0
0.5	0.0	7.4	7	0
20	0.0	7.4	13 ± 3	0
2.6	0.0	8.8	9	0
20	0.0	8.8	13	0
1.1	0.2	5.6	3	0.36
21	0.2	5.6	7	0.30
21	5.0	5.6	0	0.38

[a] Data from Figures 3–9.

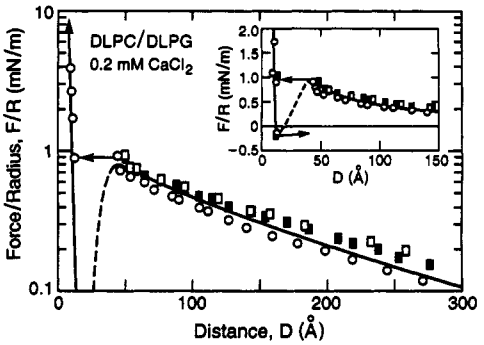

FIGURE 5: Forces between 3:1 DLPC/DLPG bilayers in 0.2 mM $CaCl_2$ at 25 °C. Interactions in one particular region of the bilayers is shown. The solid line corresponds to the actual measured data, and the position at which the surfaces jumped into adhesive contact is indicated by the arrow. The different symbols correspond to three different measurements in the same surface region but at different times. In the inset, the full force profile and the adhesive minimum are displayed on a linear plot.

The bilayer interactions at pH 8.8 were similar to those at pH 7.4 except that the steric hydration force was already evident at 9 Å in 2.6 mM NaCl (Table III). In 20 mM NaCl, a short-range repulsive force, attributed to primary and secondary hydration, dominates at separations less than 13 Å (Table III).

In none of the cases where calcium was excluded from the medium was fusion observed. Even at pressures up to ~10 atm the outer bilayer leaflets failed to undergo hemifusion. This is consistent with previous observations on fully developed phosphatidylcholine and phosphatidylglycerol bilayers (Marra, 1986b; Marra & Israelachvili, 1985).

Bilayer Interactions in the Presence of $CaCl_2$: (A) 3:1 DLPC/DLPG in 0.2 mM $CaCl_2$. In the presence of 0.2 mM $CaCl_2$, the surfaces exhibit radically different behavior than in NaCl. The behavior at different bilayer regions in a single sample (cf. Figure 13) now varied dramatically in terms of adhesive force, decay lengths, ease of fusion, and electrostatic forces. Such behavior would arise in the case of two-phase heterogeneous surfaces which may assume the form shown in Figure 13. Consequently, a region (cf. region A) consisting of a higher percentage of one phase will exhibit different interfacial behavior than a second region (cf. region B) composed of a larger percentage of the second phase. This observed behavior in the systems described here was not observed prior to the introduction of $CaCl_2$, and yet, except for the addition of $CaCl_2$, the conditions were identical to those of experiments conducted in NaCl solutions at pH 6.5. An example of this variability is shown in Figures 5 and 6. The force curve shown in Figure 5 was obtained in one region of the surfaces. Electrostatic forces dominate the long-range interaction, with the measured Debye length of 141 Å being somewhat larger than the theoretical value of 124 Å. From 38 Å there is a jump into adhesive contact at $D = 5$ Å. The

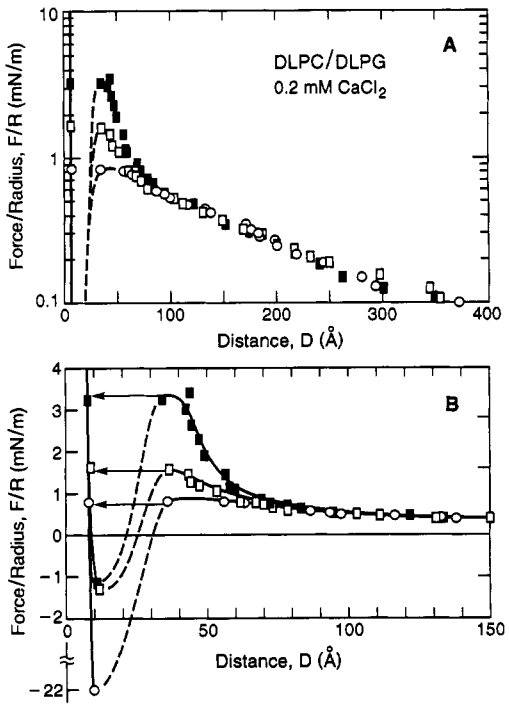

FIGURE 6: Forces between 3:1 DLPC/DLPG bilayers in 0.2 mM $CaCl_2$ at 25 °C and pH 5.6, but at a different surface region than shown in Figure 5. The different force profiles were obtained at t = 0 h (○), t = 2.5 h (□), and t = 5 h (■), demonstrating the dynamic properties of the bilayers. (A) Logarithm plot of F/R versus separation. (B) Linear plot. Positions at which the surfaces jumped into adhesive contact are indicated by arrows.

measured adhesion energies at this position were E_{ad} = 0.05 mJ/m^2 and E_{vdw} = 0.31 mJ/m^2, typical of van der Waals attraction. Fusion could not be induced in this region of the bilayer, even at large pressures. The entire force curve of Figure 5 is similar to that measured between pure DMPG bilayers in the presence of calcium (Marra, 1986b), where the adhesion at contact was also similar (depending on the NaCl concentration) but where fusion never occurred even under a high compressive force.

In contrast, Figure 6 was obtained at a second region of the same bilayer surface. As before, at 37 ± 3 Å, the surfaces jump into adhesive contact at D = 7 ± 1 Å, but the initial adhesive energy measured at this position (open circles) was E_{ad} = 4.8 mJ/m^2, nearly 10 times the van der Waals attraction and more typical of the hydrophobic force observed between depleted bilayers (Helm et al., 1989; Pashley et al., 1983; Marra & Israelachvili, 1985; Christenson et al., 1990). Furthermore, fusion now occurred readily under an applied pressure of only ~1 atm. However, the measured average thickness of the outer bilayers was unchanged, suggesting that substantial (>1 Å) bilayer thinning (or thickening) had not occurred.

In the 0.2 mM $CaCl_2$ solution, the Debye lengths varied from 117 to 145 Å depending on the bilayer regions examined. Additionally, the measured adhesive energy varied from 0.03 mJ/m^2, typical for van der Waals forces, to 5 mJ/m^2, typical of hydrophobic forces. The ease of fusion correlated directly with the strength of the hydrophobic attraction between the bilayers, consistent with previous observations (Helm et al., 1989). An estimate of the hydrophobic force at contact ($D \approx 0$) was obtained by extrapolating the data at time t = 0 (Figure 6, open circles) to D = 0, from which a value of $F_{hyd}/R \approx -25$ mN/m was obtained. Since the attractive hydrophobic force between two pure hydrophobic surfaces is −235 mN/m (Helm et al., 1992), it was estimated that 10% of the bilayer surfaces in this region were hydrophobic. Domain boundaries alone cannot account for such a large area, and some depletion/thinning of the PC-rich phase (brought about by the condensation/thickening of the PG^- lipids upon Ca binding) most likely contributes significantly to the total hydrophobic force. Note that this could occur even as the *average* thickness of the bilayers remains unchanged, as was observed.

The variation of adhesive energies, Debye lengths, ease of fusion, and electrostatic repulsion in the presence of calcium is to be contrasted with the homogeneous, position- and time-independent behavior observed on identical surfaces in the absence of calcium (cf. Figures 3 and 4) and in one-component systems of PC or PG (Marra, 1986a). Such surface heterogeneity is indicative of lateral phase separation induced by calcium. If such phase separation did occur, one would expect the behavior at a surface region to evolve over time since the DLPC/DLPG layers are expected to be fluid (Cevc & Marsh, 1987). Figure 6 demonstrates how the interaction forces at a particular region of the bilayer, held at constant temperature, changed over a period of 5 hours. Initially (open circles), the surfaces were very hydrophobic, with an adhesion energy of about 4.8 ± 0.5 mJ/m^2 (average of three measurements) and with an electrostatic double-layer repulsion that is similar to what might be expected under constant surface potential conditions. After a 2.5-h incubation following the initial contact (open squares), the adhesion energy had decreased to 0.26 ± 0.03 mJ/m^2, and fusion could now only be induced at pressures exceeding ~10 atm. The steeper increase in the electrostatic repulsion at separations less than about 70 Å is consistent with the type of force law expected if the surface charge rather than the potential remains constant during the interactions (Israelachvili, 1992). However, the observed increase in the repulsion with time is more likely to be due to the gradual decrease in the hydrophobic attraction. After an additional 2.5 h there was a further increase in the short-range repulsion (black squares) and the adhesive energy decreased slightly to about 0.23 mJ/m^2—a value that is now much closer to that expected for purely van der Waals contact.

It is significant that even though the adhesion energy gradually decreased with time while the surfaces are not in contact, it was found to increase with time (data not shown) if the surfaces were left in adhesive contact.

(B) 3:1 DLPC/DLPG in NaCl and 0.2 mM $CaCl_2$. When 1.1 mM NaCl is included in the 0.2 mM $CaCl_2$ solution at pH 5.6, the interaction profile is dominated by a long-range repulsive double-layer force (Figure 7, black circles). A short-range repulsive force due to primary hydration is evident at D < 6 Å, and the adhesion energies were E_{ad} = 0.06 mJ/m^2 and E_{vdw} = 0.72 mJ/m^2.

When NaCl was present at a concentration of 21 mM (open circles), the thickness of the outer bilayer increased by 15 Å due to increased ion binding, resulting in a larger (secondary) hydration layer. The adhesive minimum was at 17 Å, and the adhesion energy had decreased to E_{ad} = 0.04 mJ/m^2. The decreasing adhesive energy with increasing NaCl concentration and associated secondary hydration is consistent with previous measurements (Marra, 1986a; Claesson et al., 1989). Significantly, when additional $CaCl_2$ was added to bring the concentration to 5 mM (black square), the steric–hydration force was abolished, adhesive contact now occurred at D = 0, and the adhesive energy increased to E_{ad} = 0.13 mJ/m^2. This change in adhesive energy with increasing NaCl concentration and hydration is consistent with previous measurements (Marra, 1986a). The antagonistic effects of calcium and sodium ions on the interactions of charged bilayers has been observed before and is discussed later.

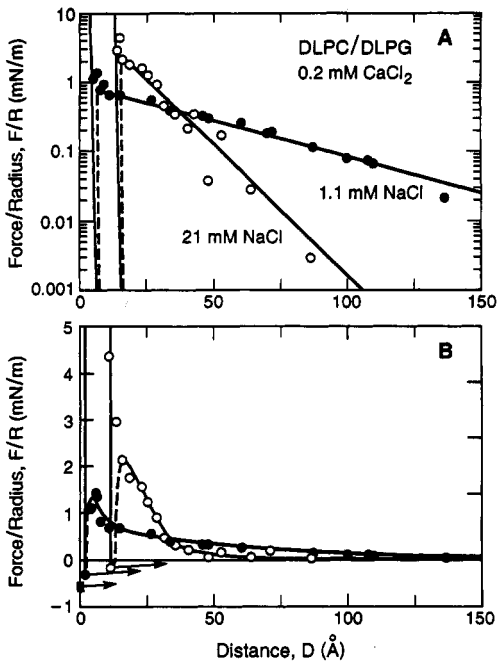

FIGURE 7: Forces between 3:1 DLPC/DLPG in the presence of 0.2 mM $CaCl_2$ in 1.1 mM (●) and 21 mM (○) NaCl at pH 5.6 and 25 °C. Following measurements at 1.1 mM NaCl (●), the solution concentration was increased to 20 mM by direct addition of a NaCl solution at pH 5.6 and 25 °C. At the end of the experiment (panel B), $CaCl_2$ was added to 5 mM (■). Arrows refer to the jump-off positions, and solid lines indicate measured data.

(C) 3:1 DLPC/DLPG in 1 mM NaCl and 2 mM $CaCl_2$. In the presence of 1 mM NaCl and 2 mM $CaCl_2$, the same variation in the forces between different bilayer regions was observed as in 0.2 mM $CaCl_2$. At some surface regions, the force profiles exhibited the usual long-range double-layer repulsion (Figure 8A). At 37 Å the surfaces jumped to adhesive contact at D = 14 Å, and the measured adhesive energy was E_{ad} = 0.11 mJ/m^2. This behavior is similar to that of pure DMPG bilayers in the presence of calcium (Marra, 1986a), though with the mixed lipid system the equilibrium contact separation is 14 Å farther out. The increased equilibrium separation distance is probably due to the steric–hydration layer of the DLPC in the outer monolayer. Previous results on pure DPPC layers at the same temperature (22 °C) show that, due to hydrated ion binding, the steric secondary hydration force extends to ~20 Å in NaCl, and primary hydration extends to 8 Å in $CaCl_2$ (Marra & Israelachvili, 1985), while between pure DPPG bilayers the steric–hydration repulsion is totally suppressed by $CaCl_2$ (Marra, 1986b; McIntosh et al., 1990). Consequently, the mixed DLPC/DLPG surfaces have characteristics intermediate between those of pure DLPC and pure DLPG, as might be expected.

At a different region, however, the electrostatic force profile is closer to constant charge interaction (Figure 8B). The curve is similar to that of Figure 6. Jumps into adhesive contact occurred from 26 Å, the equilibrium separation was closer in, at D = 2 Å, and the adhesion force was greater. The dominance of the interaction by electrostatic repulsion at large distances and the jump into contact from ~30 Å are similar to measured force profiles between fully developed, pure DLPG bilayers (Marra, 1986b).

(D) 3:1 DLPC/DLPG in 20 mM NaCl and 5 mM $CaCl_2$. In order to study the adhesion and fusion properties of the mixed bilayers under conditions similar to those used in vesicle aggregation studies, and closer to physiological conditions, the salt concentrations were increased to 20 mM NaCl and 5 mM $CaCl_2$ at pH 5.6.

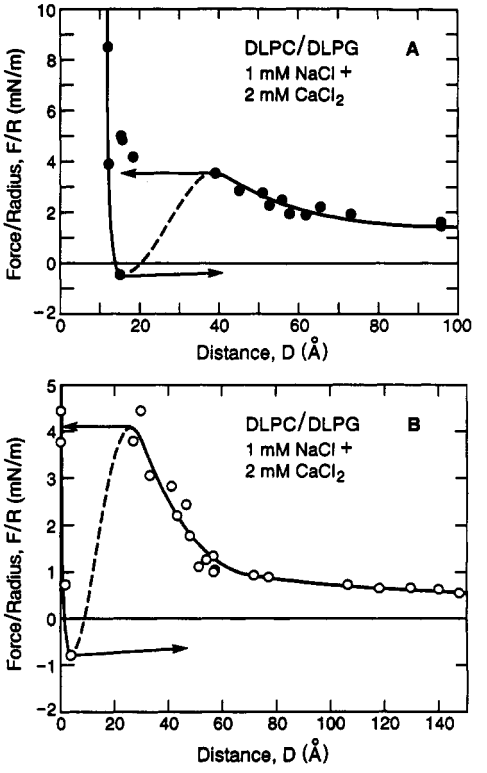

FIGURE 8: (A) Measured forces between 3:1 DLPC/DLPG bilayers in 1 mM NaCl and 2 mM $CaCl_2$ at 25 °C and pH 5.6. Forces were examined in one region of the bilayer surface. Arrows indicate the jump positions. (B) Forces measured in a second region of the same bilayer under identical conditions showing constant charge behavior.

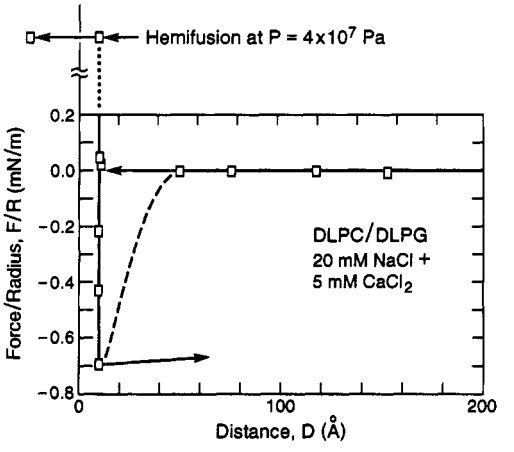

FIGURE 9: Force profile of interacting 3:1 DLPC/DLPG bilayers in 20 mM NaCl and 5 mM $CaCl_2$ at pH 5.6 and 25 °C. The solid lines indicate measured forces. The pressure at which hemifusion occurred is designated at the breakpoint.

As observed in the other experiments when calcium was present, surface heterogeneity was again evident. A typical force profile is shown in Figure 9. The interaction force was negligible until the surfaces jumped in from a distance of 42 ± 5 Å into adhesive contact at D = 5 ± 5 Å. The corresponding adhesion energy was E_{ad} = 0.15 mJ/m^2.

It was of interest to determine the pressures at which fusion occurred. According to the Hertz theory for the interaction of two deformable, nonadhering spheres, the maximum pressure in the bilayer contact region is given by (Horn et al., 1987)

$$P_{max} = \frac{1.5F}{\text{contact area}} \quad (8)$$

where F is the applied force. In Figure 9, the pressure necessary

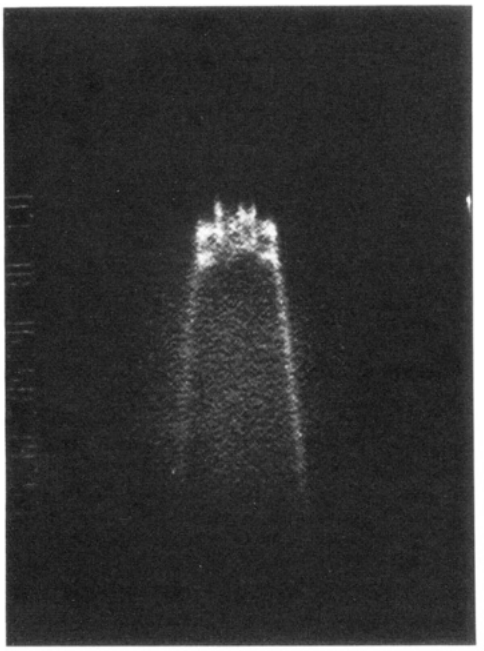

FIGURE 10: Photograph of interference fringes in the region of bilayer contact. The bilayers were 3:1 DMPC/DMPG mixtures in 20 mM NaCl and 5 mM $CaCl_2$ at pH 5.6 and 25 °C. Immobile fused patches are indicated by the projections at the front (leftmost region) of the fringe. The maximum projection corresponds to 50 Å. The vertical dimension of the protrusions correspond to 1–5 μm.

to induce fusion is indicated. The occurrence of hemifusion was highly dependent on the examined region of the bilayers. At some bilayer regions, fusion occurred at pressures above 1 atm, whereas in other regions, fusion was nearly spontaneous. The ease of fusion generally correlated with the strength of the adhesion energy: fusion was induced at pressures of 4 and 1 atm, corresponding to adhesion energies of 0.15 and 3.8 mJ/m^2, respectively. However, the measured *average* thickness of the outer bilayers always remained the same, at ~30 Å.

(E) 3:1 DMPC/DMPG in 20 mM NaCl and 5 mM $CaCl_2$. The addition of calcium to pure DMPG is known to increase the chain melting temperature to 57 °C (Marsh, 1990)—well above the temperature of the measurements (25 °C)—but calcium does not alter the phase states of DMPC or DLPC, which remain fluid at these temperatures. It was considered possible to directly observe lateral phase separation if some of the phase separated domains (e.g., DMPG-rich domains) were immobile. Though the phase diagram in Figure 2 and other calorimetric studies (Findlay & Barton, 1978) indicate that DMPG and DMPC remain miscible even in the presence of calcium, the existence of microdomains cannot be ruled out.

When DMPC/DMPG bilayers first came into adhesive contact in the presence of Ca^{2+} and Na^+, a large number of fused patches, interspersed with immobile nonfusing regions, were observed (Figure 10). The fused regions were typically a few micrometers in diameter and of thickness equal to the bilayer thickness. These data indicate that calcium simultaneously induced lateral phase separation, presumably into solidlike DMPG-rich regions and depleted fluidlike DMPC-rich regions. Fusion occurred spontaneously with no applied pressure between the fluid DMPC-rich regions.

In one region where a large concentration of fused patches was evident, the force was attractive at all separations (Figure 11, curve A) with a strongly adhesive force at $D \approx 0$ of $F/R = -3.5$ mN/m. The long-range attractive force curve could be well fitted by a double-exponential function (Claesson & Christenson, 1988; Christenson et al., 1990; Kurihara et al., 1990)

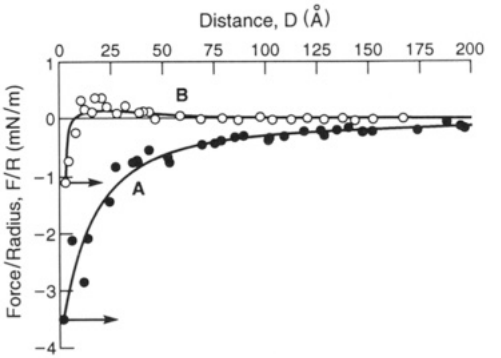

FIGURE 11: Interaction force profiles between 3:1 DMPC/DMPG bilayers in 20 mM NaCl and 5 mM $CaCl_2$ at pH 5.6 and 25 °C. The force curves was obtained by the drainage technique (Chan & Horn, 1985) at two different bilayer contact regions. The purely attractive force curve (●) was fit to eq 7, and the best-fit parameters, obtained by a nonlinear least-squares fit to the data, were $A_1 = 2.6$ mN/m, $A_2 = 0.8$ mN/m, $\lambda_1 = 18$ Å, and $\lambda_2 = 106$ Å. The solid line in the curve indicated by open circles is merely to guide the eye.

$$F/R = -(A_1 e^{-D/\lambda_1} + A_2 e^{-D/\lambda_2}) \quad (9)$$

where a least-squares fit to the data points gave $A_1 = 2.6$ mN/m, $\lambda_1 = 18$ Å, $A_2 = 0.8$ mN/m, and $\lambda_2 = 106$ Å. This behavior is typical of a hydrophobic force, which is known to exhibit a similar biphasic decay in the presence of divalent ions, characterized by long- and short-range decays lengths of 100–160 and 10–20 Å, respectively (Christenson et al., 1990; Claesson & Christenson, 1988; Kurihara et al., 1990).

In contrast, data from a different region of the same two bilayers (Figure 11, curve B) were less dominated by a hydrophobic attraction than by a (weak) double-layer repulsion, qualitatively similar to the forces seen at lower $CaCl_2$ concentrations (cf. Figures 5, 7, and 8B). The decay length of the "double-layer" repulsion was 28 Å, which is significantly larger than the theoretical value of 16 Å. A jump into adhesive contact occurs from 14 Å, and the corresponding adhesive energy is 1.2 mJ/m^2—somewhat larger than expected if only van der Waals forces were operative but less than the value measured in position A. The thickness of the fused bilayer at both positions was 52 Å.

Aggregation of Mixed 3:1 PC/PG Lipid Vesicles. In order to compare the results of force measurements with the properties of mixed 3:1 PC/PG vesicles in solution, parallel studies were conducted on the aggregation behavior of these mixed lipid vesicles in the presence of NaCl and $CaCl_2$ at pH 7.0. The dependence of vesicle aggregation on the calcium concentration at two different salt concentrations is shown in Figure 12. In a solution containing 20 mM NaCl, the calcium concentration threshold is 0.2 mM (open circles). When the NaCl is increased to 100 mM, the calcium threshold increases to about 0.6 mM (filled circles). As already mentioned (and discussed further in the Discussion), this antagonistic behavior of Na^+ and Ca^{2+} is consistent with previous ion binding and surface force measurements which show an enhancement of steric–hydration forces at higher NaCl concentrations but their suppression with $CaCl_2$. The increased calcium threshold at the higher NaCl concentration may therefore be seen as a direct consequence of the increased surface hydration due to Na^+ binding.

SUMMARY AND DISCUSSION

In earlier experiments (Marra & Israelachvili 1985; Marra, 1986a), it was found that the forces between unstressed bilayers

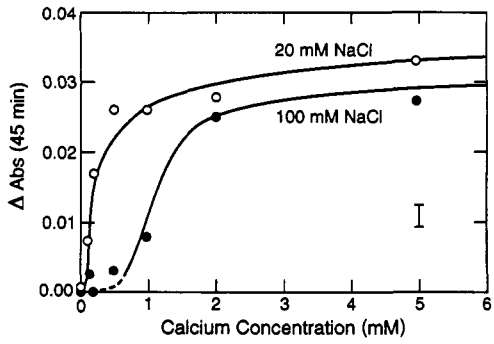

FIGURE 12: NaCl dependence of calcium thresholds for vesicle aggregation. Calcium-dependent aggregation of 3:1 PC/PG vesicles in the presence of 20 mM (○) and 100 mM (●) NaCl at pH 7.4 and 21 °C is shown. Large unilamellar vesicles were incubed with $CaCl_2$ at the indicated calcium concentrations, and vesicle aggregation was followed by turbidity changes monitored by the change in absorbance at 350 nm. The solid lines are merely to indicate measured data, and the error corresponding to all data is indicated by the error bar.

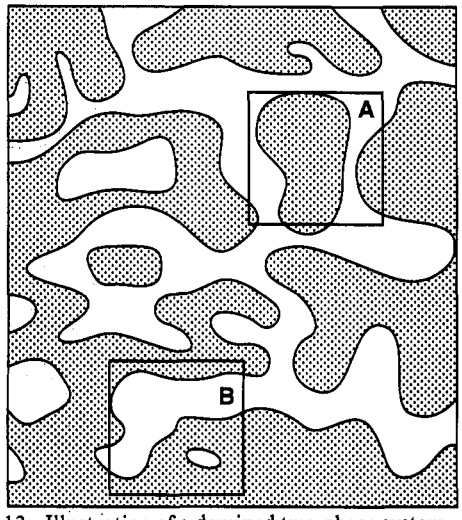

FIGURE 13: Illustration of a demixed two-phase system. The boxed regions illustrate how different surface characteristics would be measured depending on the region of the surfaces sampled by a probe with dimensions similar to the box size. For example, region A consists of more of the stippled phase and less of the plain phase. Consequently, the surface properties of this *region* will be markedly different than that of region B which contains a nearly equal proportion of the two phases.

of pure zwitterionic phospholipids (DPPC, DMPC, and DLPC) or pure ionic phospholipids (distearoyl-PG and DMPG) were well-described by the DLVO theory of attractive van der Waals and repulsive electrostatic double-layer forces. At small separations, a steric–hydration repulsion due to bound water and/or ions stabilized the van der Waals attraction at separations of $D \sim$ 10–20 Å for the PCs and at $D \sim$ 0–5 Å for the charged PG bilayers. No fusion was observed with any of these one-component bilayer systems at $CaCl_2$ concentrations up to 5 mM with bilayers in an unstressed state (e.g., not depleted or compositionally polydisperse). In contrast, pure PG vesicles aggregate but do not fuse at $CaCl_2$ concentrations up to 15 mM (Papahadjopoulos et al., 1990). However, unlike the rigidly supported bilayers used in surface forces measurements, free bilayer vesicles exposed to $CaCl_2$ often undergo large shape changes (Hui et al., 1983) and rupture, possibly resulting in fusion via different mechanisms.

The results reported here with the mixed PC/PG bilayers were initially conducted in NaCl solutions in the absence of calcium. The force curves were consistent with DLVO theory at all surface separations greater than 16 ± 3 Å, below which deviations occur due to monovalent ion binding and consequent increase in the short-range steric–hydration repulsion (Marra, 1986b; Claesson et al., 1989; Loosley-Millman et al., 1982). The measured Debye lengths and determined Hamaker constants were consistent with theory and with previous measurements (Marra & Israelachvili, 1985; Israelachvili, 1992). The surface potentials decreased with decreasing pH and increasing NaCl concentration, as expected (Claesson et al., 1989; Pashley, 1981), although the surface *charge density* increased with increasing NaCl concentration, also as predicted (Pashley, 1981; Helm et al., 1986). The force behavior was reproducible over the entire sample surface, and no anomalous behavior was observed. Fusion could not be induced under any circumstances where calcium was excluded.

From the measured effective surface charge densities in NaCl solutions it appears that only 5–10% of the charged lipids are ionized. Dissociations as low as 2–10% have previously been reported for monolayers of pure phosphatidic acid and pure dihexadecylphosphate in monovalent solutions of low ionic strength (Helm et al., 1986; Claesson et al., 1989). This behavior has been attributed to Na^+ binding to the phosphate groups (Claesson et al., 1989; Marra, 1986a). However, the analysis also assumes that the outer Helmholtz plane coincides with the theoretically defined plane of zero separation ($D = 0$). The calculated surface potentials and calculated degrees of ionization will, necessarily, depend on where the origin of surface charge lies. The presence of a Stern layer which would result from bound water or hydrated ions introduces some uncertainty in the determination of the position of the outer Helmholtz plane. The resulting force law will have the same appearance but the surface potential will be underestimated.

The effect of monovalent cation binding becomes particularly significant at higher pH values as Na^+ ions increasingly replace the hydrogen ions bound to the surfaces. Due to the larger hydration shell of the Na^+ ion, this binding results in a stronger secondary hydration repulsion (Claesson et al., 1989; Pashley, 1981; Israelachvili, 1992). The measured increase of up to 16 Å in the range of the steric–hydration force described in this work at pH > 7.4 upon NaCl addition (Table III) is entirely consistent with this trend. A similar large short-range repulsion was observed between PG multilayers at pH 7.4 in 50 mM NaCl (MacIntosh et al., 1990). In the latter case, the authors assumed that the surface potential was constant over the range of interaction. In contrast, the theoretical DLVO force law obtained if the *surface charge* is assumed constant fits the data quite well at $D >$ 6 Å (Israelachvili, 1992; Hunter, 1985). However, the sharp, steep breaks in the force laws presented here (cf. Figures 3 and 4) are inconsistent with DLVO theory, even assuming a constant charge interaction. In these measurements, the adhesion energy also decreased with increasing salt concentration, as expected. These results demonstrate that the forces between mixed lipid bilayers in NaCl, but in the absence of calcium, are consistent with current theoretical models for interacting charged colloidal surfaces where both electrostatic and hydration effects occur interdependently (Israelachvili, 1992). The apparent deviations in bilayer adhesion energies, surface charge densities, and potentials are attributed to the exchange of bound hydrated ions.

With the introduction of calcium, however, the surface properties of the bilayers were altered dramatically. The most significant change was evident in the dependence of surface characteristics on the surface region examined and on the time evolution of forces at a given region. Such surface heterogeneity has been observed between surfaces under conditions where phase separation is known to occur (Leckband

et al., 1992). The ease of fusion varied between different regions on the membrane surface, with fusion occurring easily at some regions but not at others. Additionally, in contrast to the homogeneous behavior observed in the absence of calcium, the adhesion and longer-range forces in $CaCl_2$ solutions also varied between regions. These variations include the Debye lengths (which were generally larger than expected from the DLVO theory), the magnitudes and ranges of the forces (which were generally more attractive), and the ease of fusion (which increased with increasing strength of the long-range force).

More specifically, in contrast to the force profiles in the absence of calcium, jumps into adhesive contact now occurred from larger separations (up to 40 Å), and the range of the hydration layer decreased from 16 to 0–6 Å. As expected, the final adhesion energy increased with the decreasing range of the hydration repulsion, and the adhesive force often exceeded that measured in the absence of calcium by more than an order of magnitude (Table III). The ease of fusion correlated directly with the strength of the long-range, presumed hydrophobic, attraction. For example, applied pressures of 1 and 4 atm induced fusion when the interbilayer adhesive forces were −22.6 and −7.5 mN/m, respectively. Significantly, the *average* thickness of the bilayers remained constant, in spite of the heterogeneity in their interaction behavior. The most plausible explanation for the observed heterogeneity is that calcium induces a lateral phase separation of microscopic domains in the bilayers. While the thicknesses of these domains probably differ, the average bilayer thickness is expected to remain largely unchanged.

With lipids such as DLPC and DLPG that remain fluid or fluidlike even in the presence of $CaCl_2$ at 25 °C, the heterogeneous surface morphologies of the domains would be expected to change over time. A definite time-dependent evolution in the surface forces was indeed measured, indicating that the surfaces were fluid and constantly changing. The strongly attractive "hydrophobic" force decreased with time, while the entire force profile approached the conventional DLVO type of interaction. This effect would be consistent with a slow annealing of energetically unfavorable hydrophobic patches. On the other hand, sustained interaction between *contacting* bilayers resulted in an *increased* adhesion with contact time, indicative of molecular rearrangements which maximize the hydrophobic contacts in the contact region. Upon separation, however, the adhesion energy would decrease with time as the hydrophobic components again disperse, thereby lowering the highly unfavorable surface interfacial energy.

This behavior is in sharp contrast to that observed with the same mixed bilayers in the absence of $CaCl_2$, in spite of the fact that the other conditions remain unchanged. Furthermore, studies of the interactions of pure phosphatidylcholine or pure phosphatidylglycerol in the presence and absence of calcium exhibited no such anomalies, viz., no surface heterogeneity, no fusion, and no unusual long-range attractive force (Marra & Israelachvili, 1985; Marra, 1986a; Cowley et al., 1978; Loosley-Millman et al., 1982). The enormity of the changes following the addition of $CaCl_2$ to the mixed PC/PG system can only be attributed to the effects of calcium and not to any impurities or to degradation of the system.

The likelihood that calcium induces phase separation or domain formation in bilayers was substantiated by two separate observations. First, the time evolution of the interactions (cf. Figure 6) is suggestive of surfaces that either change slowly but uniformly with time (highly unlikely) or of surfaces having different distributions of domain sizes and shapes at different positions and at different times. Given that DLPC/DLPG bilayers are expected to be in the fluid state at the temperatures of the measurements, the latter explanation appears to be more likely. Additionally, the measured increased decay lengths may also be attributed to surface heterogeneity (cf. Appendix).

Second, the appearance of immobile patches in the DMPC/DMPG bilayers (cf. Figure 10) demonstrated conclusively that calcium induces phase separation in this system. Though the phase diagrams in Figure 2 and previous calorimetric studies suggest no demixing in the presence of calcium (Findlay & Barton, 1978), these and other (Mittler-Neher, 1990) results indicate that such phase separations do occur. The discrepancy may be due to the formation of microdomains which, undectable by calorimetry or monolayer isotherms, are observable by other methods. Similar discrepancies have been noted in other mixed lipid systems (Hui et al., 1983; Helm et al., 1986).

The induction of phase separation in mixed lipid systems by calcium has been demonstrated in monolayers, in bilayer vesicles, and in black lipid membranes (Ito & Ohnishi, 1974; Miller et al., 1985; Galla & Sackmann, 1975; Mittler-Neher, 1990; Hui et al., 1983; Knoll et al., 1986; Silvius & Gagne, 1984a,b; Leventis et al., 1986). In a recent study, it was found that trace calcium impurities ($<10^{-6}$ M) were sufficient to cause phase separation a mixed dioleoyl-PC/dioleoyl-PG system above a certain mole fraction of DOPG (Mittler-Neher, 1990). In the absence of calcium, the system exhibited complete miscibility over the entire composition range, consistent with the observations reported here. The phase diagram resulting from the latter study supports the view that the systems examined in this paper separate into PG-rich and PG-poor phases upon calcium addition. Other studies with phosphatidylserine/phosphatidylcholine mixtures (Hui et al., 1983) demonstrated that calcium induces lateral phase separation and that the calcium binds to the acidic lipids. The domain sizes obtained by X-ray microprobe analysis of PS/PE vesicles were of the order of 100 Å, significantly smaller than the 1–2 μm in these measurements. The magnification of the surface forces apparatus, however, limits domain detection to ~1 μm; consequently, the existence of a large number of much smaller domains cannot be ruled out. Additionally, it is likely that the domain sizes increase slowly with time, as observed with domains in mixed monolayers at the air–water interface (Helm et al., 1986).

It has been proposed that fusion can occur at sites of packing defects in membranes and bilayers (Hui et al., 1981). Such defects might arise from local nonbilayer structures, membrane-bound proteins, impurities, or lateral phase separation (Papahadjopoulos, 1974; Hui et al., 1983). However, no evidence demonstrating a direct connection between phase separation and fusion has existed prior to these experiments.

Recent experiments demonstrated that hydrophobic forces originating from the bilayer interior were primarily responsible for the spontaneous fusion of uncharged supported bilayer membranes (Helm et al., 1989). In the experiments presented in this study, the ease of fusion correlated directly with the strength of the hydrophobic attractive force. This hydrophobic force can arise from the exposure of hydrophobic regions of the membranes, for example, at domain boundaries or in lipid-depleted regions. In the case of the mixed zwitterionic–ionic PC/PG systems studied here, it appears that calcium first causes local phase separations via its preferential binding to the anionic lipids, with subsequent area contraction in the PG-rich domains and a resulting area expansion in the PC-rich domains. More of the bilayer chain interior is thereby exposed in the fluid PC-rich domains; this renders the surfaces

more hydrophobic, resulting in a long-range hydrophobic attraction between such regions followed by their spontaneous fusion upon contact.

In this interpretation of calcium-induced bilayer fusion, the critical role of calcium is not in binding or "dehydrating" the lipid headgroups but in the induction of phase-separated domains of different lateral stresses followed by "contraction" of the (calcium/PG-rich) domains and "expansion" of the (PC-rich) domains, with the subsequent attraction and fusion of the latter. From this model it also becomes apparent why supported bilayers of pure PG (or PC) do not fuse under the same conditions: in one-component systems, the entire bilayer becomes *uniformly* stressed upon calcium binding, and thus no additional area is exposed to the aqueous phase. Consequently, enhanced hydrophobic attraction and subsequent fusion do not occur. The above interpretation appears to be consistent with the experimental data on supported bilayers. In the case of free bilayers and vesicles in solution it is likely that additional effects could occur. For example, a differential bending or bulging of the calcium-rich and calcium-poor domains may occur which cannot on the mica-supported bilayers.

Because of the complexity introduced by the surface heterogeneity, a rigorous theoretical analysis of the forces between the bilayers was not attempted; consequently, only semiquantitative statements can be made regarding the interaction. In the cases where calcium was present, the Debye lengths were larger than theoretically predicted by 50–100%. These differences are much too large to be accounted for by errors in measuring the forces or the salt concentrations. In previous force measurements between charged bilayers in the presence of calcium, measured Debye lengths were slightly smaller than predicted theoretically (Marra, 1986b), but this could be due to ion correlation forces (Kjellander & Marcelja, 1985). In the Appendix, it is demonstrated that in some cases surface charge heterogeneity may give rise to larger double-layer decay lengths than the theoretical Debye length. Similar effects and conclusions were observed in the measurements of double-layer forces between rough platinum surfaces, where an apparent increase in the decay length was associated with the distribution profile of the surface roughness (Smith et al., 1988).

The threshold concentration for calcium to induce aggregation of mixed PC/PG vesicles was found to depend on the NaCl concentration. At the NaCl concentrations employed, the increased net ionic strength due to $CaCl_2$ addition had a negligible effect on the Debye length; consequently, the increased aggregation must be attributed either to surface charge neutralization due to Ca^{2+} binding, to replacement of hydrated Na^+ by less hydrated Ca^{2+} ions on the surfaces, and/or to ion correlation effects. The force measurements reported in this work demonstrate the existence of a large surface steric–hydration layer at high NaCl concentrations, indicative of Na^+ binding. The marked increase in the calcium threshold at the higher NaCl concentration is attributed to such a secondary Na^+ hydration layer: higher calcium concentrations being required to replace the surface-bound sodium ions. Sodium binding and its effect on secondary hydration forces appear to increase with salt concentration and pH (Table II), in agreement with previous studies on both amphiphilic and nonamphiphilic surfaces (Pashley, 1981; Claesson et al., 1990; Marra, 1986a; Israelachvili, 1992).

Previous work has demonstrated that calcium-induced aggregation in mixed vesicle systems at low NaCl concentrations (<100 mM) is always followed by fusion, whereas at NaCl concentrations above 300 mM, fusion does not necessarily follow aggregation (Bentz et al., 1983). These results, too, can be attributed to the Na^+-dependent hydration layer resulting from ion binding. Calcium-induced fusion occurs at specific lipid-dependent Ca^{2+}/lipid ratios (Nir et al., 1980; Düzgunes et al., 1981; Bentz et al., 1983; Braun et al., 1985); consequently, at high Na^+ concentrations where Na^+ binding occurs, higher concentrations of calcium will be required to achieve sufficient calcium binding or sodium ejection to induce fusion. These results demonstrate the opposite effects of Ca^{2+} and Na^+ ions in the fusion mechanism. Increased Na^+ concentrations, while also decreasing the Debye length and repulsive electrostatic forces, nevertheless inhibit fusion through an increased repulsive steric–hydration force. In contrast, Ca^{2+} ions, which compete with Na^+ for anionic surface sites, also decrease the electrostatic repulsion but do not counteract this with a secondary hydration repulsion.

The calcium concentrations used in these studies were significantly greater than the micromolar quantities necessary to induce fusion in biological systems. These results, however, demonstrate the molecular effects of calcium on mixed lipid systems and the role of the Ca^{2+}-dependent alterations in fusion. Several factors in biological systems may give rise to similar phenomena under nonequilibrium conditions and on much smaller scales. Indeed, that fusion is most likely a nonequilibrium process is further evidenced by the rapid rate at which membranes reanneal following fusion. It has also been demonstrated that close apposition of membranes increases calcium binding affinity to charged bilayer surface groups (Tokutomi et al., 1981), leading to increases in the Ca^{2+}/lipid ratios, and hence fusion susceptibility, in the contact region. Reduction in calcium thresholds to physiological levels has been observed in the presence of proteins which facilitate close intermembrane contact (Düzgunes et al., 1984a,b; Düzgunes & Hoekstra, 1986; Hong et al., 1982). It has also been demonstrated that polycations induce lateral phase separation in mixed lipid systems (Galla & Sackmann, 1975), suggesting that both calcium and proteins may act cooperatively to induce local lateral phase separations.

The measurements presented in this work demonstrate the effects on intermembrane forces of local defects arising from calcium-dependent lipid packing–mismatch stresses. Measured fusion rates are much slower than the formation rates of macroscopic lipid domains (Hoekstra, 1982), but short calcium bursts between closely opposed membranes may facilitate rapid formation of localized, nonequilibrium membrane defects. This work and others (Hui et al., 1983) demonstrate that such defects need not be large to enhance fusion. Moreover, in actual biological systems, such boundary fluctuations, arising from calcium-induced lateral phase separations, will most likely be localized and occur under nonequilibrium conditions.

The most significant aspect of these experiments is the direct demonstration that monovalent and divalent cations influence the adhesion and fusion of mixed lipid bilayers through the subtle balancing of attractive and repulsive forces between different parts of a bilayer and not as a result of changes in one specific force at one point of the surface. The Ca^{2+}-dependent bilayer adhesion and fusion result from the reduction of repulsive electrostatic and hydration forces (primary and secondary) with concomitant increases in attractive hydrophobic and ion correlation forces. These attractive forces can manifest themselves at different parts of a phase-separated region. Thus, one of the implications of our findings is that fusion does not necessarily have to occur in the region of calcium binding; it can occur elsewhere where the membrane stresses propagating outward from the binding site are most

likely to be felt, for example, at a weak part of the membrane or at a point where the membrane is close to a nearby vesicle, as occurs at synaptic junctions.

In regard to the electrostatic and hydration forces responsible for the phase separation, though the presence of monovalent Na^+ ions in the solution screens the electrostatic repulsion (both between bilayers and between headgroups), this effect is more than offset by the large steric–hydration repulsion that results when Na^+ ions bind to surfaces. This hydration barrier is reduced or eliminated by replacement of hydrated Na^+ ions by less hydrated calcium ions. Consequently, Ca^{2+} and Na^+ exhibit antagonistic effects in regard to adhesion and fusion, with Na^+ having an inhibitory function.

ACKNOWLEDGMENT

We thank H. Möhwald for helpful discussions.

APPENDIX

The force between two interacting flat plates with dissimilar low potentials ($e\Psi < kT$) can be approximated by (Hunter, 1989)

$$F_d(D) = -{}^1/_2\epsilon\epsilon_0\kappa^2 \operatorname{csch}(\kappa D)\{(\psi_{01}{}^2 + \psi_{02}{}^2)\operatorname{csch}(\kappa D) - 2\psi_{01}\psi_{02}\coth(\kappa D)\} \quad \text{(A1)}$$

where ϵ and ϵ_0 are the dielectric constants of the medium and vacuum, respectively, κ^{-1} is the Debye length, and ψ_{01} and ψ_{02} are the surface potentials of surfaces 1 and 2, respectively, and $\text{sign}(\psi_{01}) = \text{sign}(\psi_{02})$. At large values of κD, this simplifies to

$$F_d(D) \approx (2\epsilon\epsilon_0\kappa^2)\psi_{01}\psi_{02}\exp(-\kappa D) = \alpha F_s(D) \quad \text{(A2)}$$

where $\alpha = \psi_{02}/\psi_{01}$ ($\alpha > 1$) and $F_s(D)$ is the interaction force between similar surfaces. Rearrangement of eq A2 gives

$$F_d(D) = 2\epsilon\epsilon_0\kappa^2\psi_{01}{}^2\exp[-\kappa(D-\delta)] \quad \text{(A3)}$$

where

$$\delta = (\ln\alpha)/\kappa \quad \text{(A4)}$$

Therefore, surface potential heterogeneity on a surface results in an effective displacement of the outer Helmholtz plane by an effective distance given by δ. Conversely, we can assume a probability distribution in δ, such that

$$dP(\delta) = \frac{\kappa}{\lambda}\exp\left(\frac{-\kappa\delta}{\lambda}\right)d\delta \quad \text{(A5)}$$

where

$$\int_0^\infty dP(\delta) = 1$$

Here λ is the assumed weighting of the distribution in δ and $\lambda > 0$. The corresponding distribution in α is obtained by differentiation of eq A4 and substitution into eq A5. The average interaction force between the two dissimilar flats can be obtained by use of eq A3 and substitution into eq A5 to obtain

$$F(D) = \frac{\beta\kappa}{\lambda}\int_0^D \exp(-\kappa D)\exp\left[-\kappa\delta\left(\frac{1}{\lambda}-1\right)\right]d\delta = \frac{\beta\exp(-\kappa D)}{(\lambda-1)}\left\{1-\exp\left[\kappa D\left(\frac{1}{\lambda}-1\right)\right]\right\} \quad \text{(A6)}$$

Here $\beta = 2\epsilon\epsilon_0\kappa^2\psi_{01}{}^2$. For $\kappa D/\lambda \ll 1$, little error is introduced by limiting the integration to the interval 0–D. The force between two curved surfaces is related to that between two flat surfaces by (Verwey and Overbeek, 1948)

$$F_c(D) = 2\pi R\int_D^\infty F(D')\,dD' \quad \text{(A7)}$$

which gives

$$F_c(D) = \frac{2\pi R\beta\exp(-\kappa D)}{\kappa(1-\lambda)}\left\{1-\lambda\exp\left[-\kappa D\left(\frac{1}{\lambda}-1\right)\right]\right\} \quad \text{(A8)}$$

In the limit of $\lambda \to 0$, $F_c(D) \to (2\pi R\beta/\kappa)\exp(-\kappa D)$, as required. As $\lambda \to 1$, $F_c(D)$ becomes $2\pi R\beta D\exp(-\kappa D)$, and the decay length is unaffected. In contrast, when $\lambda \gg 1$, eq A8 reduces to

$$F_c(D) = \frac{2\pi R\beta}{\kappa}\exp\left(\frac{-\kappa D}{\lambda}\right) \quad \text{(A9)}$$

and the apparent decay length is seen to be greater than the theoretical Debye length by a factor of λ. Therefore, the diffuseness of the outer Helmholtz plane resulting from surface heterogeneity may be ascribed to a distribution of relative potentials. If this distribution has the form given in eq A5, the resulting decay length will be increased by a factor of λ relative to the theoretical Debye length. Experimentally, values of λ as large as 2 were observed. This gives a probability of 50% for $\delta = 1.38/\kappa$, or $\alpha = 4$. Consequently, the relative average potentials in different domains on opposing surfaces appear to differ by as much as a factor of 4.

Though successful in its prediction of our observations, this model is not intended as the only possible interpretation of the origin of the long decay lengths. Other possible explanations include the existence of mobile phase domains and the presence of long-range attractive forces such as hydrophobic and ion correlation forces. The latter phenomena are also consistent with our observations.

REFERENCES

Adams, G., & Israelachvili, J. (1976) *J. Chem. Soc., Faraday Trans. 1 74*, 975–1001.

Albrecht, O., Gruler, H., & Sackmann, E. (1981) *J. Colloid Interface Sci. 79*, 319–338.

Bentz, J., Duzgünes, N., & Nir, S. (1983) *Biochemistry 22*, 3320–3330.

Birdi, K. S. (1989) *Lipid and Bipolymer Monolayers at Liquid Interfaces*, Plenum Press, New York.

Boni, L. T., & Hui, S. W. (1987) in *Cell Fusion* (Sowers, A. E., Ed.) Plenum Press, New York.

Braun, G., Lelkes, P., & Nir, S. (1985) *Biochim. Biophys. Acta 812*, 688–694.

Cevc, G., & Marsh, D., Eds. (1987) *Phospholipid Bilayers: Physical Principles and Methods*, John Wiley and Sons, New York.

Chan, D., Healy, T., & White, L. (1976) *J. Chem. Soc., Faraday Trans. 1 72*, 2844–2865.

Chan, D. Y. C., & Horn, R. G. (1985) *J. Chem. Phys. 83*, 5311–5324.

Chen, Y. L., Helm, C. A., & Israelachvili, J. N. (1991) *J. Phys. Chem. 95*, 10736–10747.

Christenson, H., Fang, J., Ninham, B., & Parker, J. (1990) *J. Phys. Chem. 94*, 8004–8006.

Claesson, P., & Christenson, H. (1988) *Science 239*, 390–392.

Claesson, P. M., Herder, P. C., Berg, J. M., & Christenson, H. K. (1990) *J. Colloid Interface Sci. 136*, 541–551.

Claesson, P., Carmona-Ribeiro, A. M., & Kurihara, K. (1989) *J. Phys. Chem. 93*, 917–922.

Cowley, A. C., Fuller, N., Rand, P., & Parsegian, A. (1978) *Biochemistry 17*, 3163–3168.

Duzgünes, N., & Hoekstra, D. (1986) *Stud. Biophys. 111*, 5–10.

Duzgünes, N., Nir, S., Wilschut, J., Bentz, J., Newton, C., Portis, A., & Papahadjopoulis, D. (1981) *J. Membr. Biol. 59*, 115–125.

Duzgünes, N., Paiement, J., Freeman, K. B., Lopez, N., Wilschut, J., & Papahadjopoulos, D. (1984a) *Biochemistry 23*, 3486–3494.

Duzgünes, N., Hoekstra, D., Hong, K., & Papahadjopoulos, D. (1984b) *FEBS Lett. 173*, 80–84.
Evans, E., & Metcalfe, M. (1984) *Biophys. J. 46*, 423–425.
Feigenson, G. (1986) *Biochemistry 25*, 5819–5825.
Findlay, E. J., & Barton, P. G. (1978) *Biochemistry 17*, 2400–2405.
Galla, H. J., & Sackmann, E. (1975) *J. Am. Chem. Soc. 97*, 4114–4120.
Helm, C. A., Laxhuber, M., Lösche, M., & Möhwald, H. (1986) *Colloid Polym. Sci. 264*, 46–55.
Helm, C. A., Möhwald, H., Kjaer, K., & Als-Nielson, J. (1987) *Europhys. Lett. 4*, 697–703.
Helm, C. A., Israelachvili, J., & McGuiggan, P. (1989) *Science 246*, 919–922.
Helm, C. A., Israelachvili, J., & McGuiggan, P. (1992) *Biochemistry 31*, 1794–1805.
Hoekstra, D. (1982) *Biochemistry 21*, 2833–2840.
Hong, K., Duzgünes, N., & Papahadjopoulos, D. (1982) *Biophys. J. 37*, 296–305.
Horn, R., Israelachvili, J., & Pribac, F. (1987) *J. Colloid Interface Sci. 115*, 480–493.
Hui, S. W., Stewart, T. P., Boni, L. T., & Yeagle, P. L. (1981) *Science 212*, 921–923.
Hui, S. W., Boni, L. T., Stewart, T., & Isaac, T. (1983) *Biochemistry 22*, 3511–3516.
Hunter, R. J. (1989) *Foundations of Colloid Science*, Clarendon Press, Oxford, England.
Israelachvili, J. N. (1973) *J. Colloid Interface Sci. 44*, 259–272.
Israelachvili, J. (1992) *Intermolecular Forces*, 2nd ed., Academic Press, New York.
Israelachvili, J., & Wennerström, H. (1992) *J. Phys. Chem. 96*, 520–531.
Ito, T., & Ohnishi, S. I. (1974) *Biochim. Biophys. Acta 352*, 29–37.
Johnson, K. L., Kendall, K., & Roberts, A. D. (1971) *Proc. R. Soc. London A. 324*, 301–313.
Kjellander, R., & Marcelja, S. (1985) *Chem. Scr. 25*, 112–116.
Knoll, W., Apell, H. J., Eible, H., & Miller, A. (1986) *Eur. Biophys. J. 13*, 187–193.
Knoll, W., Schmidt, G., Rötzer, H., Henkel, T., Pfeiffer, W., Sackmann, E., Mittler-Neher, S., & Spinke, J. (1991) *Chem. Phys. Lipids 57*, 363–374.
Kurihara, K., Kato, S., & Kunitake, T. (1990) *Chem. Lett.*, 1555–1558.
Leckband, D., Schmitt, F.-J., Knoll, W. C., & Israelachvili, J. (1992) *Science, 255*, 1419–1421.
Leiken, S., Kozlov, M., Chernomordik, L., Markin, V., & Chizmdzhev, Y. (1987) *J. Theor. Biol. 129*, 411–425.
Leventis, R., Gagné, J., Fuller, N., Rand, P., & Silvius, J. (1986) *Biochemistry 25*, 6978–6987.
Lis, L. J., McAlister, M., Fuller, N., Rand, R. P., & Parsegian, V. A. (1982) *Biophys. J. 37*, 657–666.
Loosley-Millman, M., Rand, P., & Pasegian, V. (1982) *Biophys. J. 40*, 221–232.
MacDonald, R. C., & Simon, S. A. (1987) *Proc. Natl. Acad. Sci. U.S.A. 84*, 4089–4094.
Marra, J. (1986a) *Biophys. J. 49*, 815–825.
Marra, J. (1986b) *J. Phys. Chem. 90*, 2145–2150.
Marra, J., & Israelachvili, J. (1985) *Biochemistry 24*, 4608–4618.
Marra, J., & Israelachvili, J. (1986) *Methods Enzymol. 127*, 353–360.
Marsh, D. (1990) *Handbook of Lipids*, CRC Press, Boca Raton, FL.
McIntosh, T. J., Magid, A. D., & Simon, A. (1990) *Biophys. J. 57*, 1187–1197.
McIver, D. J. L. (1970) *Physiol. Chem. Phys. 11*, 289–302.
Miller, A., Schmidt, G., Eible, H., & Knoll, W. (1985) *Biochim. Biophys. Acta 813*, 221–229.
Mittler-Neher, S. (1990) Ph.D. Thesis, Universität Mainz, Mainz, FRG.
Mittler-Neher, S., & Knoll, W. (1989) *Biochem. Biophys. Res. Commun. 162*, 124–129.
Mittler-Neher, S., & Knoll, W. (1990) *Biochim. Biophys. Acta 1026*, 167–170.
Nir, S., Bentz, J., & Portis, A. R. (1980) *Adv. Chem. Soc. 188*, 75–106.
Ohki, S. (1982) *Biochim. Biophys. Acta 689*, 1–11.
Ohki, S., & Duzgünes, N. (1979) *Biochim. Biophys. Acta 552*, 438–439.
Ohki, S., & Ohshima, H. (1984) *Biochim. Biophys. Acta 776*, 177.
Papahadjopoulos, D., Poste, G., Schaeffer, B. E., & Vail, W. J. (1974) *Biochim. Biophys. Acta 352*, 10–28.
Papahadjopoulos, D., Vail, W., Pangborn, W., & Poste, G. (1976) *Biochim. Biophys. Acta 448*, 265–283.
Papahadjopoulos, D., Vail, W. J., Newton, C., Nir, S., Jacobson, K., Poste, G., & Lazo, R. (1977) *Biochim. Biophys. Acta 465*, 579–598.
Papahadjopoulos, D., Portis, A., Panghorn, W., & Newton, C. (1978) in *Transport of Macromolecules in Cellular Systems* (Silverstein, S. C., Ed.) pp 413–430, Dahlem Konferenzen, Berlin.
Papahadjopoulos, D., Nir, S., & Duzgünes, N. (1990) *J. Bioeng. Biomembr. 22*, 157–179.
Parsegian, A., & Rand, P. (1983) *Ann. N.Y. Acad. Sci. 416*, 1–12.
Pashley, R. (1981) *J. Colloid Interface Sci. 80*, 153–162.
Portis, A., Newton, C., Pangborn, W., & Papahadjopoulos, D. (1979) *Biochemistry 18*, 780–790.
Poste, G., & Nicolson, G. L., Eds. (1984) *Membrane Fusion*, Elsevier/North-Holland, Amsterdam.
Rand, P. (1981) *Annu. Rev. Biophys. Bioeng. 10*, 277–314.
Rand, P., & Parsegian, V. (1986) *Annu. Rev. Physiol. 48*, 201–212.
Servuss, R. M., & Helfrich, W. (1989) *J. Phys. (Paris) 50*, 809.
Siegel, D., Banschbach, J., Alford, D., & Ellens, H. (1989) *Biochemistry 28*, 3703–3709.
Silvius, J., & Gagné, J. (1984a) *Biochemistry 23*, 3232–3240.
Silvius, J., & Gagné, J. (1984b) *Biochemistry 23*, 3241–3247.
Smith, C. P., Maeda, M., Atanososka, L., White, H. S., & McClure, D. J. (1988) *J. Phys. Chem. 92*, 199–205.
Sowers, A. E., Ed. (1987) *Cell Fusion*, Plenum Press, New York.
Szoka, F., & Papahadjopoulos, D. (1978) *Proc. Natl. Acad. Sci. U.S.A. 75*, 4194–4198.
Tanford, C. (1972) *J. Phys. Chem. 93*, 917–922.
Tokutomi, S., Lew, R., & Ohnishi, S. (1981) *Biochim. Biophys. Acta 643*, 276–282.
Verwey, E. J. W., & Overbeek, J. Th. (1948) *Theory of the Stability of Lyophobic Colloids*, Elsevier, Amsterdam.